Biosensors and Bioelectronics 133 (2019) 147–153

Contents lists available at ScienceDirect

Biosensors and Bioelectronics

journal homepage: www.elsevier.com/locate/bios

Label-free detection of *Staphylococcus aureus* bacteria using long-period fiber gratings with functional polyelectrolyte coatings

Fan Yang[a], Tzu-Lan Chang[b], Tianchi Liu[b], Di Wu[a], Henry Du[a], Junfeng Liang[b], Fei Tian[a,*]

[a] Department of Chemical Engineering and Materials Science, Stevens Institute of Technology, Hoboken, NJ 07030, United States
[b] Department of Chemistry and Chemical Biology, Stevens Institute of Technology, Hoboken, NJ 07030, United States

ARTICLE INFO

Keywords:
Long-period fiber gratings
Biosensing
Staphylococcus aureus
Polyelectrolyte
Antibody-antigen
Nanopitted coatings

ABSTRACT

Highly sensitive long-period fiber gratings (LPFG) was developed for label-free and rapid detection of *Staphylococcus aureus (S. aureus)*. Specifically, the LPFG was functionalized with antibody and nanopitted polyelectrolyte coatings to facilitate bacterial adhesion and thus enhance the sensitivity of bacteria detection. The kinetics of *S. aureus* adhesion on functional coatings were tracked by surface morphology evolution and time-resolved resonance wavelength shift of the coated LPFG at a flow rate of 30 μl/ml and 37 °C in the concentration range of 10^4–10^8 colony forming unit (CFU)/ml. *S. aureus* detection at concentrations as low as 224 CFU/ml can be achieved within a short time span of 30 min. The LPFG-based biosensor can be readily adapted to a variety of biophotonic platforms, for applications such as food safety inspection, environmental monitoring, clinical diagnostics, and medical applications.

1. Introduction

S. aureus is one of the most common pathogens responsible for diverse disease symptoms including skin, soft-tissue, and systemic infections in humans and animals (Deurenberg and Stobberingh, 2008). In the pre-antibiotic era, it was associated with a high incidence of mortality: 10–30% of these patients would die from *S. aureus* bacteremia. *S. aureus* infection accounts for a greater number of deaths than AIDS, tuberculosis, and viral hepatitis combined (van Hal et al., 2012). *S. aureus* is a dynamic and adaptable bacterium that has a remarkable ability to acquire strong antibiotic resistance quickly (Pantosti et al., 2007). Rapid detection of this pathogenic bacterial strain is thus crucial to avoid a major microbial mediated infection and outbreaks, to help maintain a healthy environment and to improve public health in a timely manner.

Biochemical assays have been widely used for *S. aureus* detection, in addition to the gold standard of traditional culturing methods in pathogen diagnosis. Each of these methods has its own advantages and disadvantages. For example, bacterial cell culture conducted prior to most biochemical assays normally takes 6–8 h to obtain a sufficient number of bacterial cells. And the subsequent recognition of the nucleic acid, though offering high specificity, suffers from the inability to discriminate between viable and non-viable cells (Dorst et al., 2010). In the fluorescent-label method, the recognition elements have to be labeled with specific dyes, making this procedure complex, time-consuming and possible alteration of the properties of the analyte (Goodridge et al., 1999). In the field of biochemical and biomedical sensing, label-free optical biosensors are increasingly drawing attention for the ability in fast, reliable and in-situ measurements (Wolfbeis, 2006). Among optics-based detection methods, surface plasmon resonance (SPR)-based biosensor is most commonly used for the detection of *S. aureus* (Bo et al., 1983; Subramanian et al., 2006; Tawil et al., 2012), in spite of its limited sensor area and mass transport limitations (Helmerhorst et al., 2012). Long-period fiber gratings has recently been used for biological analyte detection (Bandara et al., 2015; Bock et al., 2015) because of their high sensitivity in comparison to other platforms, in addition to low cost, simple fabrication processes and robustness in harsh environments. As a refractive index transduction platform, LPFG not only allows the quantitative measurement of the investigated analyte but also provides unique opportunity to analyze the dynamic interactions in biochemical processes with the aid of functional coatings deposited on the surface (Chiavaioli et al., 2014).

In this study, an LPFG-based optofluidic platform is developed for the rapid and reliable detection of *S. aureus* at low concentrations. We explored an in-situ layer-by-layer (LbL) deposition technique to secure high-quality functional coatings deposited on fiber surface with strong adhesion as well as thickness control. Polyelectrolyte functional coatings were subsequently modified to selectively facilitate the bacterial

* Corresponding author.
E-mail addresses: fyang7@stevens.edu (F. Yang), tchang2@stevens.edu (T.-L. Chang), tliu7@stevens.edu (T. Liu), dwu8@stevens.edu (D. Wu), hdu@stevens.edu (H. Du), jliang2@stevens.edu (J. Liang), ftian1@stevens.edu (F. Tian).

https://doi.org/10.1016/j.bios.2019.03.024
Received 23 January 2019; Received in revised form 13 March 2019; Accepted 13 March 2019
Available online 14 March 2019
0956-5663/

adhesion on the surfaces. The functional coatings not only significantly increase the initial rate of bacterial adhesion onto the surfaces, but also dramatically improve the sensitivity of LPFG and thus the detection limit for *S. aureus* bacteria. The adhesion kinetics and affinity between bacteria and functional coatings were studied to estimate the initial rate of bacterial adhesion and quantify the capacity of functional coatings for the initial bacterial adhesion. We demonstrated a linear-log correlation between the resonance wavelength of the coated LPFG and bacterial concentration in a time span of 30 min. The limit of bacteria detection on antibody-immobilized nanopitted polyelectrolyte coatings was estimated to be 224 CFU/ml based on the linear-log fitting model and the spectral resolution of coated LPFG.

2. Experimental section

2.1. $[PAH/PAA]_{10}$-PAH coatings

The LPFG was mounted straight between two holders on an optical stage. It was dipped into a container with a V-shaped groove containing polyelectrolyte solutions during the LbL assembly. Briefly, the LPFG was cleaned with 7.5% H_2O_2 solution for 20 min before LbL deposition. Polyelectrolyte coatings were deposited at room temperature by alternately dipping the fiber in the V-shaped groove containing positively charged PAH solution for 5 min followed by two consecutive rinsing steps in 100 mM buffer solution for 2 min, and then into a negatively charged PAA solution for 5 min followed by the same rinsing cycle. The solutions were injected and aspirated by syringes. The entire deposition process was repeated 10 times, establishing a polyelectrolyte coating of $[PAH/PAA]_{10}$-PAH on the surface of LPFG. All polyelectrolyte solutions and rinsing buffer were pH-adjusted to 6.0 during the deposition process. When the deposition process was completed, the coated LPFG was immersed in the PBS solution at pH 7.5 until the coatings were stabilized and subsequently dried in an oven at 200 °C.

2.2. Pitted $[PAH/PAA]_{10}$-PAH coatings

The $[PAH/PAA]_{10}$-PAH coatings prepared in Section 2.1 were immersed into the acidic solution of pH 2.4 for 60 s, rinsed with the neutral water of pH 7.5 for about 15 s, blown dry, and then dried at 200 °C in an oven for 1 h. Both the nonpitted and pitted coatings were stored under ambient conditions prior to measurement.

2.3. Immobilization of antibody on pristine and $[PAH/PAA]_{10}$-PAH coated LPFG

The LPFG was cleaned by immersion in 200 ml of 5% nitric acid for 2 h at 90 °C followed by thorough rinse in deionized water. Silanization of the LPFG surface was performed by immersion in 200 ml of fresh 10% (v/v) APTES in water (pH 3–4) for 1 h at 75 °C. The treated LPFG was dried in a convection oven for 4 h at 115 °C. After cooling, both the silanized and $[PAH/PAA]_{10}$-PAH coated LPFG were treated with 1% (v/v) glutaraldehyde in water (pH 6–7) for 30 min at room temperature. After rinsing in 0.01 M PBS solution (pH 7.5) for 15 min, the treated LPFG was incubated in 2 ml of 0.5 mg/ml *Staphylococcus aureus* antibody in 10 mM sodium acetate (pH 5.4) overnight at 4 °C. Once immobilization of antibody was completed, the LPFG was inserted into a quartz capillary to form the microfluidic device assembly.

2.4. Surface characterization and analysis

The size of nanopits and attached bacteria on the functional coatings were studied using a Scanning Electron Microscope (SEM), Auriga Modular Cross Beam workstation (Carl Zeiss, Inc.) with 3 kV accelerating voltage. The density of *S. aureus* bacteria (numbers per mm^2) on functional coatings was analyzed on the SEM images using ImageJ software.

To determine the coverage density of antibody on functional coatings, 2D fluorescence images of FITC-labeled antibody were achieved by a confocal microscope (Nikon E1000 with NikonC1-Plus confocal system), then analyzed by ImageJ software. The coverage density of antibody was defined as the ratio: $A_{antibody}/A_{surface}$, where $A_{antibody}$ is the surface area covered by antibody, and $A_{surface}$ is the area of the entire surface.

2.5. Detection principle and the optofluidic platform

LPFG enables the coupling of the propagating core mode and co-propagating cladding modes. The high attenuation of the cladding modes results in a series of attenuation bands centered at discrete wavelengths in the transmission spectrum, with each attenuation band corresponding to a specific cladding mode. The phase matching condition between the guided mode and the forward propagating cladding modes is given by $\beta_{01} - \beta_{cl}^{(n)} = \frac{2\pi}{\Lambda}$, where Λ is the grating period, β_{01} and $\beta_{cl}^{(n)}$ are the propagation constants for the fundamental core mode and the n^{th} cladding mode, respectively. The effective refractive indices of the core and cladding are obtained by $n_{eff,co} = \frac{\beta_{01}\lambda}{2\pi}$ and $n_{eff,clad}^{(n)} = \frac{\beta_{cl}^{(n)}\lambda}{2\pi}$, respectively. The resonance wavelength (RW) is thus obtained by $\lambda_{res} = (n_{eff,co} - n_{eff,clad}^{(n)})\Lambda$ (Vengsarkar et al., 1996). The dependence of λ_{res} on $n_{eff,co}$ and $n_{eff,clad}^{(n)}$ makes LPFG a highly sensitive index transduction platform.

We designed and developed an innovative all-optical lab-on-fiber optofluidic platform (LOFOP) for in-situ measurements in the biologically and physiologically relevant microenvironment. It consists of two key and multi-functional components. One component is the LPFG structure. The other component is a glass capillary to mimic microenvironment as well as to allow the bacterial adhesion on LPFG. The LPFG and the glass capillary (length = 5 cm, I.D. = 1.56 mm) are assembled to form liquid-tight LOFOP with inlet and outlet for flow regulation by a syringe pump. To avoid thermal and tension cross-talk effects, the coated LPFG was mounted in LOFOP with two ends fixed and the entire LOFOP was in an incubator maintained at ~37 °C. The various concentrations of *S. aureus* in PBS solution were delivered into the LOFOP via a syringe pump (New Era Pump Systems, Inc.) at a flow rate of 30 μl/ml, seen in Scheme S1. The transmission spectra of coated LPFG in the optofluidic platform were continuously monitored every ten minutes in sets of bacterial concentrations of 10^4–10^8 CFU/ml for up to 8 h.

3. Results and discussion

3.1. Surface morphology of pitted polyelectrolyte coatings

PAH and PAA have been widely used in cell/film studies (Lichter et al., 2008; Gribova et al., 2012; Yang et al., 2017). The pitted structure in the PAH/PAA coating with a size comparable to that of *S. aureus* was fabricated to facilitate the adhesion of more bacteria on the surface. Pits were observed to protect cells or bacteria from chemicals and hydrodynamic shear forces (Perera-Costa et al., 2014) in the fluidic condition, further promoting *S. aureus* adhesion on the pitted coatings and thus enhancing the sensitivity of LPFG to *S. aureus*.

A substantial and irreversible transformation could take place in the topography of PAH/PAA coatings by the pH-introduced method in an acidic solution to generate either nanopitted or nanoporous structure (Mendelsohn et al., 2000). Pitted $[PAH/PAA]_{10}$-PAH coatings can thus be fabricated on the LPFG by acid treatment after initial LbL assembly. Fig. 1(a) shows the pitted coating with the size of nanopits ranging from 200 nm to 1.6 μm. As depicted in Fig. 1(b), the average diameter of these nanopits on the pitted $[PAH/PAA]_{10}$-PAH coatings is around 800 ± 192 nm, which closely matches the physical profile of *S. aureus* ATCC 29213.

As illustrated in Scheme S2, a two-step mechanism for the formation

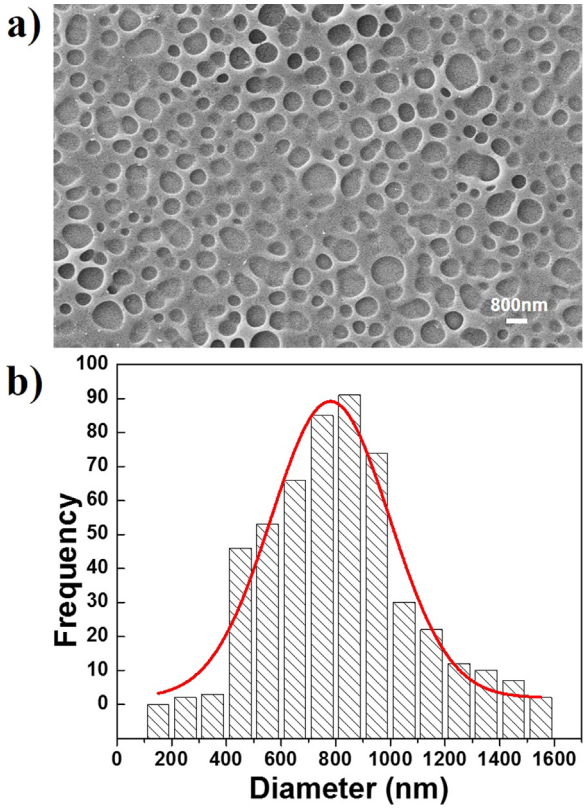

Fig. 1. (a) The SEM image of pH-induced pitted $[PAH/PAA]_{10}$-PAH coating on LPFG; (b) Statistical histogram displays the diameter distribution of the nanopits on the $[PAH/PAA]_{10}$-PAH coatings.

of pits in PAH/PAA coatings is proposed. These transformations are based on interchain ionic bond breakage. The new nanopit transition is associated with a partial breaking of the interchain ion-pairs in the first step, which are formed in the highly protonating environment. In the second step, the resultant reorganization of the polymer chains produces an insoluble polyelectrolyte complex that phase separates from the neutral solution, yielding a classical spinodally decomposed morphology (Mendelsohn et al., 2000). It was noticed that both the pH of the acid solution and the molecular weight of PAA influence the size of nanopits. Comparing with PAH/(PAA, 120 kDa) coatings, the size of nanopits in PAH/(PAA, 1250 kDa) coatings are improved 2 times. PAA with larger molecular weight possesses more charged groups so that more interchain ionic bonds of PAH/PAA coatings are broken in acid solution. Therefore, more highly swollen complex in the coatings is formed to cause larger size of nanopits in neutral solution.

3.2. Antibody immobilization

The antigens of *S. aureus* specifically form higher affinity bond with the specific antibodies via antigen-antibody complex (Osato, 1972). Therefore, the antigen-antibody interaction helps facilitate bacterial adhesion on the surface of antibody immobilized LPFG. FITC-labeled *S. aureus* antibody was initially attached on the untreated LPFG by physisorption, and weak intensity of fluorescence signals and low coverage density are observed after rinse in PBS solution, as shown in Fig. S1(a). For comparison, the silanized LPFG is used to improve the antibody immobilization. As shown in Fig. S1(b), there is a higher fluorescence intensity. A clear optical fiber profile is observed. The difference in fluorescence intensity along the radial direction is attributed to different focal length on the circular surface of the optical fiber. The inset in Fig. S1(b) clearly shows that the antibody has been successfully immobilized on the fiber surface. As shown in Fig. S1(c), the antibody had been bonded with $[PAH/PAA]_{10}$-PAH coated LPFG and the relevant average coverage density is 86 ± 3%. Fig. S1(d) also shows that the antibody has been immobilized successfully on the surface of pitted $[PAH/PAA]_{10}$-PAH coatings and the average coverage density was calculated to be 70 ± 5%. Interestingly, when the fluorescence microscope focused on the surface of $[PAH/PAA]_{10}$-PAH coatings, the shape of nanopits is partially defined by the contrast of fluorescence intensity in Fig. S1(d) that is due to the difference in focal lengths between the surface and nanopits.

All samples prior to fluorescence microscopy were rinsed in PBS buffer solution for 3 times. Comparing to the coverage of antibody in Fig. S1(a), the higher coverage in Fig. S1(b-d) indicates better stability and durability of immobilized antibody, due to the stronger interaction of the covalent bonds between the antibody and coated LPFG.

3.3. Stability of functional coatings on LPFG

The RW of LPFG with various functional coatings is recorded at a flow rate of 30 μl/ml in the PBS solution (37 °C) for 8 h in order to examine the stability of the functional coatings. Fig. S2 illustrates that the functional coatings on LPFG are stable with a maximum RW fluctuation of 0.05 nm, which is comparable to the resolution of OSA (0.05 nm). The stability of $[PAH/PAA]_{10}$-PAH and pitted $[PAH/PAA]_{10}$-PAH coatings is attributed to the chemical cross-linking by means of a thermally induced amidization reaction. These coatings were heated up to 200 °C after the fabrication to form amide crosslinks (–NHCO–) between COO^- groups of PAA and NH_3^+ groups of PAH (Harris et al., 1999). Even though PAH and PAA are responsive to ionic strength in the PBS solution, the concentration of ionic strength is low and nearly constant. LPFG with PAH/PAA coatings was soaked in the PBS solution for 10 min until RWs became constant. The covalent bonds by the thermal/chemical reaction between antibody and PAH/PAA coatings account for the stability and durability of the coated LPFG in fluidic and physiologically relevant conditions.

All RWs of LPFG with functional coatings increased as shown in Fig. S2, comparing to that of the pristine LPFG. The RW shift was attributed to the increase of cladding effective refractive index induced by higher RI coatings and consequently the phase-matching condition was tuned. Red-shift (i.e. increase in wavelength) in RWs, in this case, indicates increased thickness of the functional coatings on the LPFG (Yang et al., 2017). Fig. S2 also shows that the immobilized antibody increased the effective refractive index of the coatings, resulting in red-shifts in RWs. And the pitted structure reduced refractive index of the PAH/PAA coatings, resulting in blue-shifts (i.e. decrease in wavelength) in RWs compared to the LPFG with nonpitted PAH/PAA coatings.

3.4. The adhesion capacity of S. aureus on LPFG with functional coatings

The real-time RW shifts of LPFG with functional coatings were monitored every 10 min for 8 h in 10^4 CFU/ml *S. aureus* PBS solution at a flow rate of 30 μl/ml and 37 °C, as shown in Figs. 3–5. SEM images of *S. aureus* on LPFG with functional coatings after 30 min are shown in Fig. 2. The densities of *S. aureus* on various functional coatings were estimated, as shown in Fig. S3. Fresh *S. aureus* solution was continuously injected into the LOFOP microfluidic device by a syringe pump system. The refractive index of the *S. aureus* solution surrounding the coated LPFG did not change, assuming that the concentration of *S. aureus* was constant in a short time span of 1 h (Vaamonde and Chirife, 1986). The shifts in RW ($\Delta\lambda_{res}$) are due to the increased surface refractive index of LPFG, indicating a gradual bacterial adhesion on the surface of coated LPFG.

The real-time $\Delta\lambda_{res}$ measurements allow us to explore and explain the kinetics of bacterial adhesion on various functional coatings on the LOFOP. The $\Delta\lambda_{res}$ of coated LPFG was recorded in the first hour and then analyzed by the regression analysis. The slope of the linear $\Delta\lambda_{res}$ is defined as the initial rate of bacterial adhesion that reliably evaluates

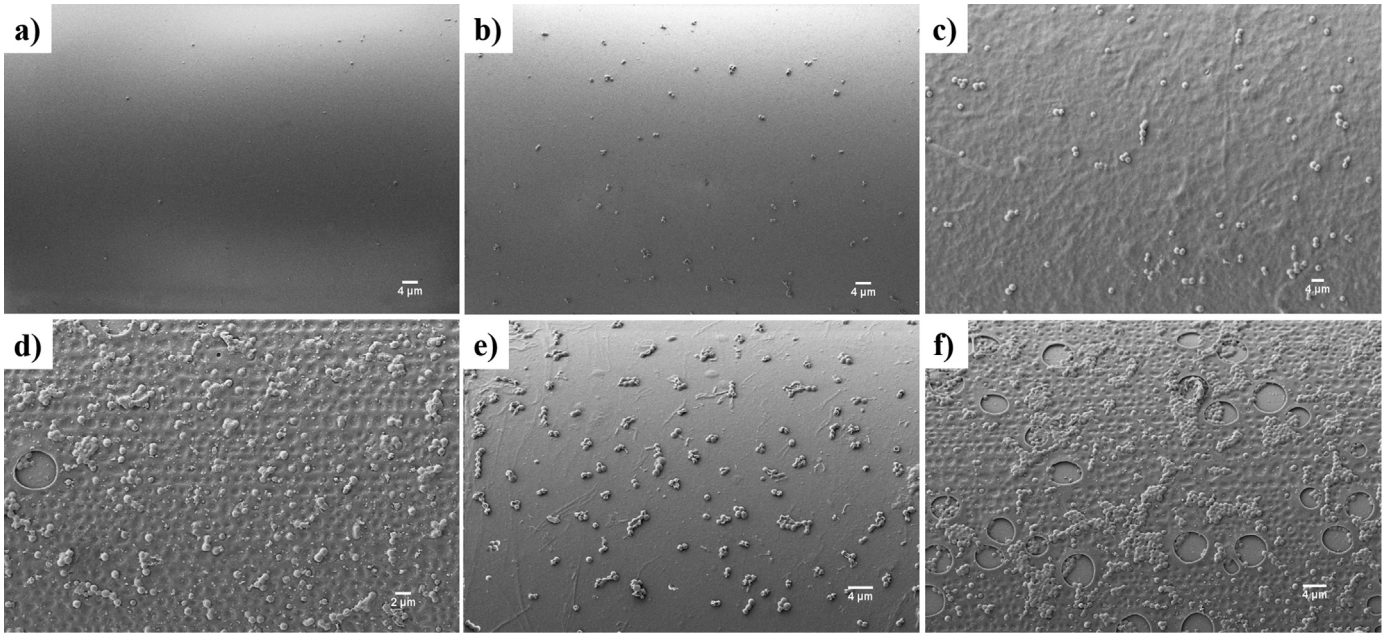

Fig. 2. SEM images of *S. aureus* on various functional coatings on LPFG after 30 min in 10^4 CFU/ml bacteria PBS solution at a flow rate of 30 μl/ml and 37 °C: (a) the pristine LPFG, (b) immobilized antibody, (c) $[PAH/PAA]_{10}$-PAH, (d) pitted $[PAH/PAA]_{10}$-PAH, (e) $[PAH/PAA]_{10}$-PAH-antibody, (f) pitted $[PAH/PAA]_{10}$-PAH-antibody.

and characterizes the adhesion of *S. aureus* bacteria on various functional coatings.

3.4.1. Pitted LbL coatings – LbL coatings

S. aureus is negatively charged, and it more readily colonizes on positively charged surface (An and Friedman, 2002). As positively charged groups (Gribova et al., 2012), the amine groups of the PAH-terminated coatings improve the initial attachment of *S. aureus* via electrostatic interaction (Zhu et al., 2016). Meanwhile, the thickness of $[PAH/PAA]_n$-PAH coatings can also be altered by layer numbers (n) and pH value of polymer solutions during LbL assembly (Thompson et al., 2005). In this study, the $[PAH/PAA]_{10}$-PAH coating was assembled at pH 6 in order to obtain the suitable stiffness for subsequent *S. aureus* adhesion (Lichter et al., 2008).

The initial rate of bacterial adhesion on the $[PAH/PAA]_{10}$-PAH coating is 2.57 times in average larger than that on the pristine LPFG in 4 times of measurements (shown in Table S1), indicating the enhancement of bacterial adhesion with the functional coatings. Because of the increasing rate of bacterial adhesion in pitted $[PAH/PAA]_{10}$-PAH coating, the $\Delta\lambda_{res}$ and slope of pitted $[PAH/PAA]_{10}$-PAH coated LPFG are larger than that of $[PAH/PAA]_{10}$-PAH coated LPFG, respectively, as shown in Fig. 3(a). Based on the slopes in Fig. 3(b), the initial rate of bacterial adhesion increased 3.7 times on pitted $[PAH/PAA]_{10}$-PAH coatings compared to that without pits. The pitted structure with the optimal size of nanopits in PAH/PAA coatings tends to increase the overall surface area and reduces the shear stress experienced by attached bacteria in the fluidic condition, so that recessed portions of the nanopitted surface is in favor for bacterial adhesion (Palmer et al., 2007; Renner and Weibel, 2011; Berne et al., 2018). Fig. 2(d, f) clearly shows that a fraction of the bacteria lie in the pits of pitted $[PAH/PAA]_{10}$-PAH coatings. Fig. S3 shows that the density of *S. aureus* on functional coatings with pitted structure are higher than that on the pristine LPFG, further demonstrating that pitted structure effectively enhances the bacterial adhesion thus the sensitivity of LPFG.

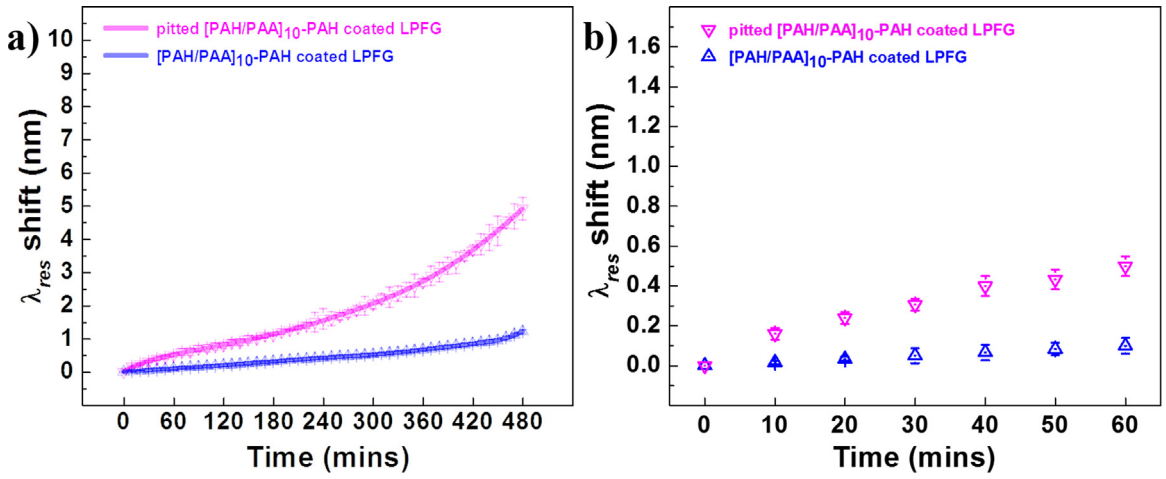

Fig. 3. The time-resolved λ_{res} shift of LPFG coated with $[PAH/PAA]_{10}$-PAH and pitted $[PAH/PAA]_{10}$-PAH in 10^4 CFU/ml *S. aureus* PBS solution for (a) 480 min and (b) 60 min.

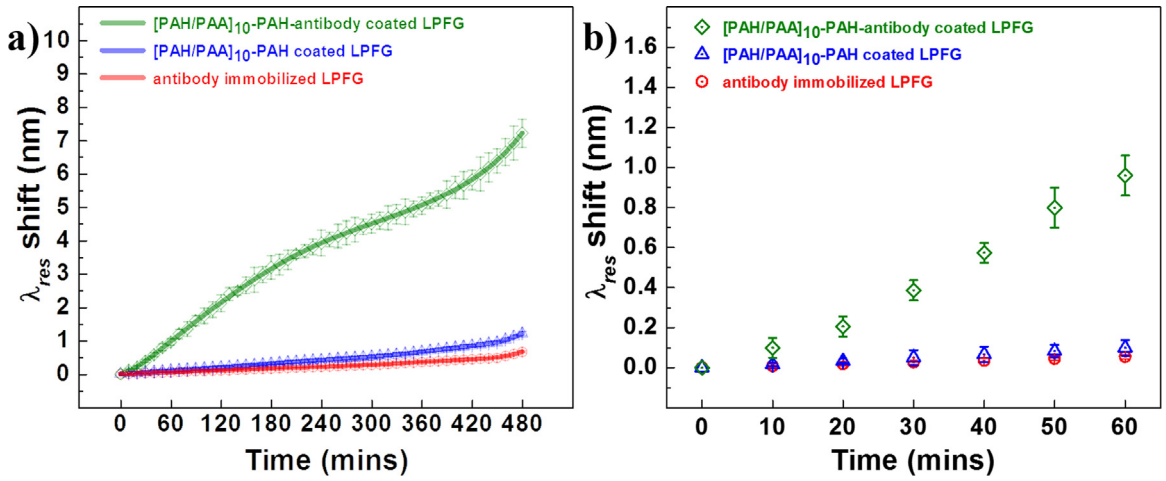

Fig. 4. The time-resolved λ_{res} shift of LPFG coated with antibody, $[PAH/PAA]_{10}$-PAH and $[PAH/PAA]_{10}$-PAH-antibody in 10^4 CFU/ml *S. aureus* PBS solution for (a) 480 min and (b) 60 min.

3.4.2. Immobilized antibody – LbL coatings

The immobilized antibody attracts bacteria efficiently and selectively via the antigen-antibody interaction (Dryla et al., 2005). The initial rate of bacterial adhesion on LPFG immobilized with antibody is 0.91 ± 0.08 pm/min, which is 2 times of that of the pristine LPFG, as shown in Table S1. The $\Delta\lambda_{res}$ of LPFG immobilized with antibody is close to that of the $[PAH/PAA]_{10}$-PAH coatings in Fig. 4, compared with that of $[PAH/PAA]_{10}$-PAH-antibody coatings. Interestingly, the initial rate of bacterial adhesion on $[PAH/PAA]_{10}$-PAH-antibody coatings is 9-fold and 17-fold higher than that of bacterial adhesion on LPFG with either $[PAH/PAA]_{10}$-PAH or antibody, respectively. SEM image in Fig. 2(e) and density of *S. aureus* in Fig. S3 show that more *S. aureus* are attached on $[PAH/PAA]_{10}$-PAH-antibody coatings in comparison with the other two coatings (Fig. 2(b, c)). The synergy effect of the antibody and PAH/PAA coatings for the improvement of bacterial adhesion can be attributed to the increased coverage density of antibody, the antibody is immobilized not only on the surface but also between the layers of PAH/PAA coatings.

3.4.3. Pitted LbL coatings – immobilized antibody

The remarkable initial rate of bacterial adhesion on pitted $[PAH/PAA]_{10}$-PAH-antibody coatings is 28.13 ± 0.09 pm/min, which is 0.7-fold, 2.5-fold and 60-fold higher than that of bacterial adhesion on $[PAH/PAA]_{10}$-PAH-antibody, pitted $[PAH/PAA]_{10}$-PAH coatings and the surface of pristine LPFG, respectively. Comparing with the other coatings in Fig. 2 and Fig. S3, the maximum density of *S. aureus* on pitted $[PAH/PAA]_{10}$-PAH-antibody coatings is consistent with its largest λ_{res} shift (Fig. 5(a)) and highest initial rate of bacterial adhesion (Fig. 5(b)) on the same coating at 30 min. This improvement in bacterial adhesion is due to the biochemical binding of the antigen-antibody complex, electrostatic attraction, and the nanopitted structure with the suitable size for *S. aureus* as a habitation in the fluidic condition. The combination of antibody and pitted structure dramatically enhances the sensitivity of LPFG for *S. aureus* detection at a low concentration of 10^4 CFU/ml in a short time span. The sensitivity of the pitted $[PAH/PAA]_{10}$-PAH-antibody coated LPFG is 0.478 ± 0.005 nm/log (CFU/ml), which is 8 times higher than 0.053 ± 0.032 nm/log (CFU/ml) of the pristine LPFG. The *S. aureus* antibody as bio-receptor has specificity to *S. aureus* (Selle et al., 2016) and the pitted structure with the round shape and suitable size can potentially resist the adhesion of other bacteria with different outlines, such as *E. coil* (Helbig et al., 2016; Lu et al., 2016). It is expected that the antibody immobilized pitted polyelectrolyte coatings possess the selectivity for the detection of *S. aureus* in principle. Further studies are required to explore this possibility.

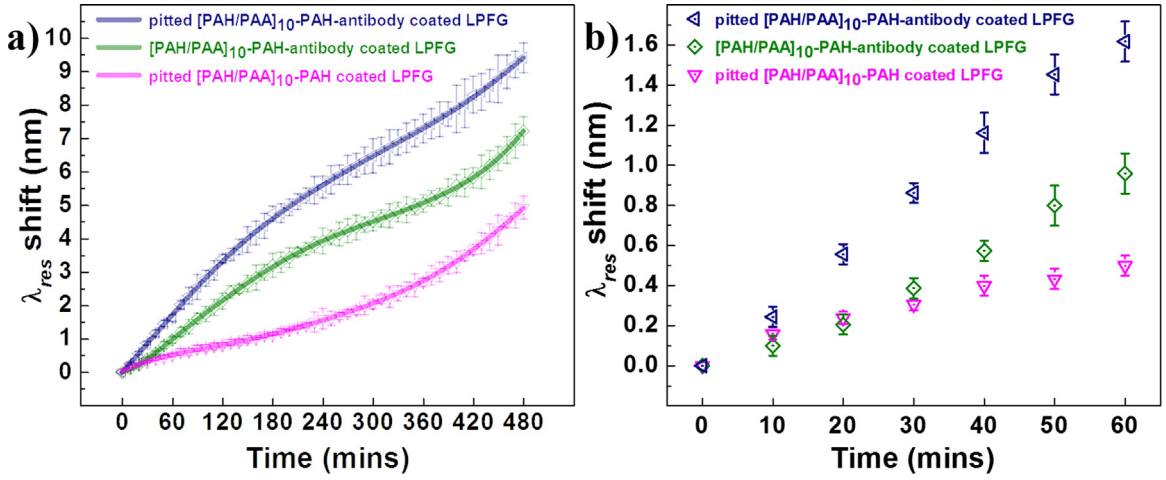

Fig. 5. The time-resolved λ_{res} shift of LPFG coated with $[PAH/PAA]_{10}$-PAH, $[PAH/PAA]_{10}$-PAH-antibody and pitted $[PAH/PAA]_{10}$-PAH-antibody coatings in 10^4 CFU/ml *S. aureus* PBS solution for (a) 480 min and (b) 60 min.

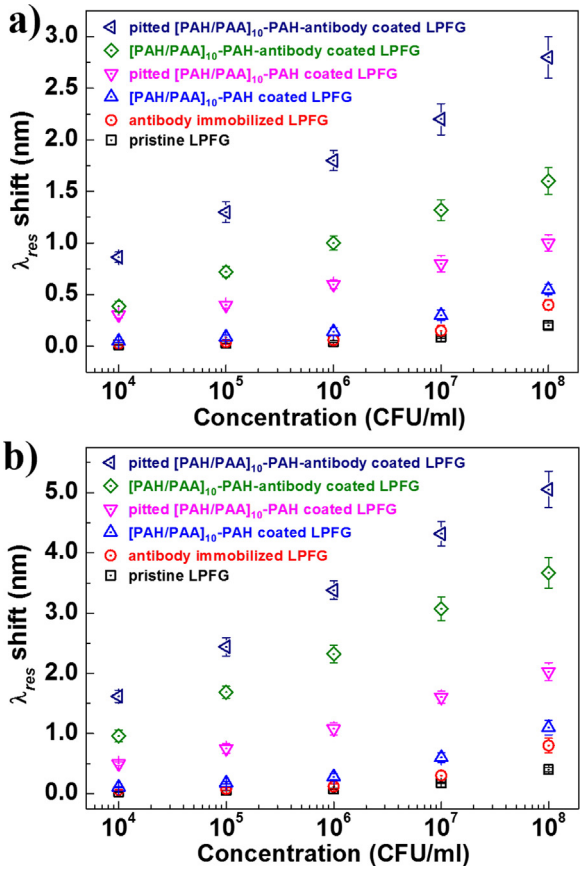

Fig. 6. λre_s shifts of LPFG coated with functional coatings from 10^4 to 10^8 CFU/ml *S. aureus* PBS solution at a flow rate of 30 μl/ml and 37 °C at (a) 30 min and (b) 60 min.

3.5. S. aureus detection with functionalized LPFG

The $\Delta\lambda_{res}$ of various functional coatings on LPFG was recorded three times in the *S. aureus* PBS solution with the concentrations of 10^4–10^8 CFU/ml. For rapid detection, the $\Delta\lambda_{res}$ of coated LPFG at 30 and 60 min in various *S. aureus* concentrations is shown in Fig. 6(a) and (b), respectively. A linear-log model is used with a logarithmic scale in x-axis and a linear scale in y-axis to explore the correlation between the RW of LPFG and the concentration of *S. aureus*. The linear-log regression relationships between $\Delta\lambda_{res}$ and corresponding concentrations of *S. aureus* solution are both calculated at 30 and 60 min in Fig. 6. The best fitting of the experimental data is represented as $\Delta\lambda_{res}$ = Slope × log (Concentration) + Intercept, making quantification of measured bacterial concentration straightforward. Note that the slope is defined as the sensitivity of the functionalized LPFG-based biosensor.

For the pitted $[PAH/PAA]_{10}$-PAH-antibody coated LPFG at 30 min, the RW shifts were 0.86 ± 0.05, 1.32 ± 0.11, 1.83 ± 0.12, 2.31 ± 0.15 and 2.82 ± 0.21 nm for *S. aureus* concentrations of 10^4, 10^5, 10^6, 10^7, 10^8 CFU/ml, respectively, as shown in Fig. 6(a). The relevant slope of its fitting curve was calculated to be 0.478 ± 0.005 nm/log(CFU ml^{-1}), and the linear-log equation is $\Delta\lambda_{res}$ = 0.478 × log (Concentration) −1.073, (R^2 = 0.99). As a result, the $\Delta\lambda_{res}$ of this coated LPFG at 30 min is estimated to be 0.36 nm if the concentration is 10^3 CFU/ml. With a spectral resolution of 0.05 nm (OSA), the achieved limit concentration of detection (LOD) can be 224 CFU/ml, which is 44 times higher than that of the pristine LPFG. The sensitivity and LOD of other coatings on LPFG are solved and shown in Table S2. The sensitivity and LOD in short time span are determined by the initial rate of bacterial adhesion on functional coatings, which is the dominating factor of sensitivity in bacteria detection.

All 60-min curves of coated LPFG in Fig. 6(b) exhibit slopes nearly 2 times as large as that of 30-min curves in Fig. 6(a), indicating that the bacterial adhesion is still increasing at 60 min for concentration as high as 10^8 CFU/ml with no saturation effect. Basically, better sensitivity and LOD could always be achieved by increasing time for bacterial adhesion. Comparing to the performance of the pristine LPFG in various concentrations of *S. aureus*, the functional coatings on the LPFG significantly improve the sensitivity for detection in short time span by facilitating the bacterial adhesion on the surface of coated LPFG.

4. Conclusion

A highly sensitive label-free biosensor for rapid detection of *S. aureus* has been demonstrated using LPFG integrated with functional coatings. The LbL technique allows deposition of high-quality and uniform thickness coatings on LPFG surface. The polyelectrolyte coatings with pitted structure and immobilized antibody were designed and fabricated to facilitate the *S. aureus* attachment and increase the initial rate of bacterial adhesion on the series of functional coatings, in order to improve the surface refractive index increment surrounding the LPFG. Therefore, the growth of the sensitivity is proportional to the increasing time-resolved λ_{res} shift of coated LPFG. The kinetics of bacterial adhesion on the functional coatings have been explored by the time-resolved RW of coated LPFG, which provides the theoretical framework for further development of LPFG-based *S. aureus* sensors. According to the linear-log range of the concentration between 10^4 and 10^8 CFU/ml at a short detection time of 30 min, the sensitivity of pitted $[PAH/PAA]_{10}$-PAH-antibody coated LPFG is 0.478 ± 0.005 nm/log (CFU/ml), corresponding to a detection limit of 224 CFU/ml. The detection limit and sensitivity are 84-fold and 10-fold better than that of the pristine LPFG, respectively. This detection limit is 2–10-fold lower than that those achieved using surface plasmon resonance-based sensors (Tawil et al., 2012; Balasubramanian et al., 2007; Chen et al., 2007). Our optofluidic LPFG sensing scheme with functional coatings provides an attractive bioanalytical platform for *S. aureus* detection. Importantly, our approach offers numerous advantages such as ease of fabrication, high sensitivity, label-free, real-time monitoring, and good stability.

CRediT authorship contribution statement

Fan Yang: Conceptualization, Methodology, Software, Validation, Formal analysis, Investigation, Data curation, Writing - original draft, Writing - review & editing, Visualization, Supervision. **Tzu-Lan Chang:** Methodology, Investigation, Writing - review & editing. **Tianchi Liu:** Investigation, Data curation. **Di Wu:** Software, Investigation. **Henry Du:** Writing - review & editing, Resources, Supervision, Project administration, Funding acquisition. **Junfeng Liang:** Writing - review & editing, Resources, Supervision. **Fei Tian:** Formal analysis, Conceptualization, Writing - review & editing, Resources, Supervision, Project administration, Funding acquisition.

Acknowledgment

This work is supported by the US National Science Foundation under grant number ECCS-1611155.

Declaration of interests

The authors declare that they have no known competing financial interests or personal relationships that could have appeared to influence the work reported in this paper.

Appendix A. Supporting information

Supplementary data associated with this article can be found in the

online version at doi:10.1016/j.bios.2019.03.024.

References

An, Y.H., Friedman, R.J., 2002. Concise review of mechanisms of bacterial adhesion to biomaterial surfaces. J. Biomed. Mater. Res. 43, 338–348.

Balasubramanian, S., Sorokulova, I.B., Vodyanoy, V.J., Simonian, A.L., 2007. Lytic phage as a specific and selective probe for detection of Staphylococcus aureus—a surface plasmon resonance spectroscopic study. Biosens. Bioelectron. 22, 948–955.

Bandara, A.B., Zuo, Z., Ramachandran, S., Ritter, A., Heflin, J.R., Inzana, T.J., 2015. Detection of methicillin-resistant staphylococci by biosensor assay consisting of nanoscale films on optical fiber long-period gratings. Biosens. Bioelectron. 70, 433–440.

Berne, C., Ellison, C.K., Ducret, A., Brun, Y.V., 2018. Bacterial adhesion at the single-cell level. Nat. Rev. Microbiol. 16, 616–627.

Bo, L., Claes, N., Ingemar, L., 1983. Surface plasmon resonance for gas detection and biosensing. Sens. Actuators 4, 299–304.

Bock, W.J., Tripathi, S.M., Smietana, M., 2015. Sensitive and selective lab-on-a-fiber sensor for bacteria detection in water. In: Cusano, A., Consales, M., Crescitelli, A., Ricciardi, A. (Eds.), Lab-on-Fiber Technology. Springer International Publishing, Cham, pp. 301–313.

Chen, L., Deng, L., Liu, L., Peng, Z., 2007. Immunomagnetic separation and MS/SPR end-detection combined procedure for rapid detection of Staphylococcus aureus and protein A. Biosens. Bioelectron. 22, 1487–1492.

Chiavaioli, F., Biswas, P., Trono, C., Bandyopadhyay, S., Giannetti, A., Tombelli, S., Basumallick, N., Dasgupta, K., Baldini, F., 2014. Towards sensitive label-free immunosensing by means of turn-around point long period fiber gratings. Biosens. Bioelectron. 60, 305–310.

Deurenberg, R.H., Stobberingh, E.E., 2008. The evolution of Staphylococcus aureus. Infect. Genet. Evol. 8 (8), 747–763.

Dorst, B. Van, Mehta, J., Bekaert, K., Rouah-martin, E., Coen, W., De, Dubruel, P., Blust, R., Robbens, J., 2010. Recent advances in recognition elements of food and environmental biosensors: a review. Biosens. Bioelectron. 26, 1178–1194.

Dryla, A., Prustomersky, S., Gelbmann, D., Hanner, M., Bettinger, E., Meinke, A., Nagy, E., 2005. Comparison of Antibody Repertoires against Staphylococcus aureus in Healthy Individuals and in Acutely Infected Patients 12, 387–398.

Goodridge, L., Chen, J., Griffiths, M., 1999. Development and characterization of a fluorescent-bacteriophage assay for detection of *Escherichia coli* O157:H7. Appl. Environ. Microbiol. 65, 1397–1404.

Gribova, V., Auzely-Velty, R., Picart, C., 2012. Polyelectrolyte multilayer assemblies on materials surfaces: from cell adhesion to tissue engineering. Chem. Mater. 24, 854–869.

Harris, J.J., DeRose, P.M., Bruening, M.L., 1999. Synthesis of passivating, nylon-like coatings through cross-linking of ultrathin polyelectrolyte films. J. Am. Chem. Soc. 121, 1978–1979.

Helbig, R., Günther, D., Friedrichs, J., Rößler, F., Lasagni, A., Werner, C., 2016. The impact of structure dimensions on initial bacterial adhesion. Biomater. Sci. 4, 1074–1078.

Helmerhorst, E., Chandler, D.J., Nussio, M., Mamotte, C.D., 2012. Real-time and label-free bio-sensing of molecular interactions by surface plasmon resonance: a laboratory medicine perspective. Clin. Biochem. Rev. 33, 161–173.

Lichter, J.A., Thompson, M.T., Delgadillo, M., Nishikawa, T., Rubner, M.F., Vliet, K.J. Van, 2008. Substrata mechanical stiffness can regulate adhesion of viable bacteria. Biomacromolecules 1571–1578.

Lu, N., Zhang, W., Weng, Y., Chen, X., Cheng, Y., Zhou, P., 2016. Fabrication of PDMS surfaces with micro patterns and the effect of pattern sizes on bacteria adhesion. Food Control 68, 344–351.

Mendelsohn, J.D., Barrett, C.J., Chan, V.V., Pal, A.J., Mayes, A.M., Rubner, M.F., 2000. Fabrication of microporous thin films from polyelectrolyte multilayers. Langmuir 16, 5017–5023.

Osato, K., 1972. Antigen-antibody complexes in the immune response. Immunology 23, 545–557.

Palmer, J., Flint, S., Brooks, J., 2007. Bacterial cell attachment, the beginning of a biofilm. J. Ind. Microbiol. Biotechnol. 34, 577–588.

Pantosti, A., Sanchini, A., Monaco, M., 2007. Mechanisms of antibiotic resistance in Staphylococcus aureus. Future Microbiol. 2, 323–334.

Perera-Costa, D., Bruque, J.M., González-Martín, M.L., Gómez-García, A.C., Vadillo-Rodríguez, V., 2014. Studying the influence of surface topography on bacterial adhesion using spatially organized microtopographic surface patterns. Langmuir 30, 4633–4641.

Renner, L.D., Weibel, D.B., 2011. Physicochemical regulation of biofilm formation. MRS Bull. 36, 347–355.

Selle, M., Hertlein, T., Oesterreich, B., Klemm, T., Kloppot, P., Müller, E., Ehricht, R., Stentzel, S., Bröker, B.M., Engelmann, S., Ohlsen, K., 2016. Global antibody response to Staphylococcus aureus live-cell vaccination. Sci. Rep. 6, 24754.

Subramanian, A., Irudayaraj, J., Ryan, T., 2006. Mono and dithiol surfaces on surface plasmon resonance biosensors for detection of Staphylococcus aureus. Sens. Actuators, B Chem. 114, 192–198.

Tawil, N., Sacher, E., Mandeville, R., Meunier, M., 2012. Surface plasmon resonance detection of *E. coli* and methicillin-resistant S. aureus using bacteriophages. Biosens. Bioelectron. 37, 24–29.

Thompson, M.T., Berg, M.C., Tobias, I.S., Rubner, M.F., Van Vliet, K.J., 2005. Tuning compliance of nanoscale polyelectrolyte multilayers to modulate cell adhesion. Biomaterials 26, 6836–6845.

Vaamonde, G., Chirife, J., 1986. Effect of phosphate buffer on Staphylococcus aureus growth at a reduced water activity. Int. J. Food Microbiol. 3, 51–55.

van Hal, S.J., Jensen, S.O., Vaska, V.L., Espedido, B.A., Paterson, D.L., Gosbell, I.B., 2012. Predictors of Mortality in Staphylococcus aureus Bacteremia. Bacteremia. Clin. Microbiol. Rev. 25, 362–386.

Vengsarkar, A.M., Lemaire, P.J., Judkins, J.B., Bhatia, V., Erdogan, T., Sipe, J.E., 1996. Long-period fiber gratings as band-rejection filters. J. Light. Technol. 14, 58–65.

Wolfbeis, O.S., 2006. Fiber-optic chemical sensors and biosensors. Anal. Chem. 78, 3859–3874.

Yang, F., Sukhishvili, S., Du, H., Tian, F., 2017. Marine salinity sensing using long-period fiber gratings enabled by stimuli-responsive polyelectrolyte multilayers. Sens. Actuators, B Chem. 253, 745–751.

Zhu, X., Guo, S., He, T., Jiang, S., Jańczewski, D., Vancso, G.J., 2016. Engineered, robust polyelectrolyte multilayers by precise control of surface potential for designer protein, cell, and bacteria adsorption. Langmuir 32, 1338–1346.